# Pyrene-Terminated Phenylenethynylene Rigid Linkers Anchored to Metal Oxide Nanoparticles

**Olena Taratula, Jonathan Rochford, Piotr Piotrowiak, and Elena Galoppini***

*Chemistry Department, Rutgers University, 73 Warren Street, Newark, New Jersey 07102*

**Rachael A. Carlisle and Gerald J. Meyer***

*Department of Chemistry and Department of Materials Science and Engineering, Johns Hopkins University, 3400 North Charles Street, Baltimore, Maryland 21218*

*Received: April 18, 2006; In Final Form: June 13, 2006*

Phenylenethynylene (PE) rigid linkers (para and meta) were used to anchor pyrene to the surface of $TiO_2$ (anatase) and $ZrO_2$ nanoparticle thin films through the two COOH groups of an isophthalic acid (Ipa) unit. Four chromophore-linker models were studied in solution and bound. Two are novel *meta*-pyrene−PE linker systems: dimethyl 5-(3-(1-pyrenylethynyl)phenylethynyl)-isophthalate, carrying one pyrene, and dimethyl 5-(bis-3,5-(1-pyrenylethynyl)phenylethynyl)-isophthalate, carrying two. These were compared with para rigid-rods dimethyl 5-(1-pyrenylethynyl)isophthalate and dimethyl 5-(4-(1-pyrenylethynyl)phenylethynyl)-isophthalate, each carrying one pyrene but varying in length. The length of the PE linkers and the para or meta substitution influence the photophysical properties of the compounds. The extinction coefficient increased, and the long wavelength absorbance of the pyrene chromophore was shifted to the red with increasing conjugation. Compared to unsubstituted pyrene, the pyrene-linker systems were characterized by short fluorescence lifetimes ($\tau \sim 2$ ns in tetrahydrofuran solutions), but quantum yields were close to unity. ZINDO/S CI calculations attribute this effect to a switching in the order of the two lowest-lying singlet states of pyrene. High surface coverages, $\sim 10^{-8}$ mol/cm$^2$, and carboxylate binding modes on nanostructured $TiO_2$ films were obtained in all cases. The appearance of a pyrene excimer emission on $ZrO_2$, an insulator, indicates that the pyrene-linker system is closely packed (Py−Py < 4 Å) on the surface. The fluorescence emission on $TiO_2$ was completely quenched, consistent with quantitative and rapid electron injection into the semiconductor indicating that the pyrene excimer acts as a sensitizer. Photoelectrochemical studies in regenerative solar cells with $I_3^-/I^-$ as the redox mediator indicated near-quantitative conversion of absorbed photons into an electrical current.

## Introduction

The development of photosensitizing chromophores for the study of dye−semiconductor interfaces is one of the most exciting areas of scientific research.[1] Molecules that anchor a chromophore to the surface of semiconductor nanoparticles through rigid linkers[2] (for instance, tripods[3,4] and rigid-rods[4−6]) that are made of a variable number of phenylenethynylene (PE) units are useful models for fundamental studies of interfacial electron injection.[3c,5b,c] We have recently described rigid-rods with pyrene as the organic chromophore, PE units as the spacer, and isophthalic acid (Ipa) as the anchoring group.[5b] Pyrene was selected because the long-lived $S_1$ state (650 ns in nonpolar media)[7] and favorable redox potentials are well-suited for semiconductor sensitization. Long excited-state lifetimes ensure that charge injection is complete, even at the largest distances between the chromophore and the nanoparticle. Preliminary work on pyrene rigid-rods has shown that the conjugated PE units in the linker significantly influenced the photophysical properties of pyrene, both in solution and anchored to colloidal $TiO_2$ films.[5b] As the number of PE units increased, the extinction coefficient increased, the absorbance shifted to the red, and the lifetime decreased by about 2 orders of magnitude compared to that of unsubstituted pyrene. The photophysical properties of PE oligomers have been recently reported.[8] Preliminary data with regenerative solar cells with two pyrene rigid-rod sensitizers indicated that the PE spacer dramatically improved the optical properties of 1-pyrene carboxylic acid, an inefficient sensitizer for $TiO_2$ solar cells, leading to efficient solar cells.[5b]

Surprisingly, this improvement occurred despite an increase in the sensitizer−semiconductor distance and a dramatic decrease in the pyrene excited-state lifetime. In addition, recent studies of ethynyl derivatives of pyrene[9] indicate that ethynylpyrenes have near-unity fluorescence quantum yields and may be useful as laser dyes.[9a−c] In summary, pyrene rigid-rods with PE spacers combine promising photoelectrochemical properties with an unusual photophysical behavior that deserves further investigation.[9]

In this paper, we study the PE linker effects by comparing the series of pyrene-linker compounds **1**−**4** in Figure 1. Novel compounds that contain meta derivatives were also included. Recent studies have shown that meta conjugation can increase the lifetime of the charge-separated excited state of conjugated PE systems by decreasing the efficiency of charge recombination.[9f] Photophysical, photoelectrochemical, and electrochemical studies of **1**−**4** have been complemented with quantum mechanical

* Corresponding author. E-mail: galoppin@andromeda.rutgers.edu (E.G.); meyer@jhu.edu (G.J.M.).

10.1021/jp0623847 CCC: $33.50 © 2006 American Chemical Society
Published on Web 07/27/2006

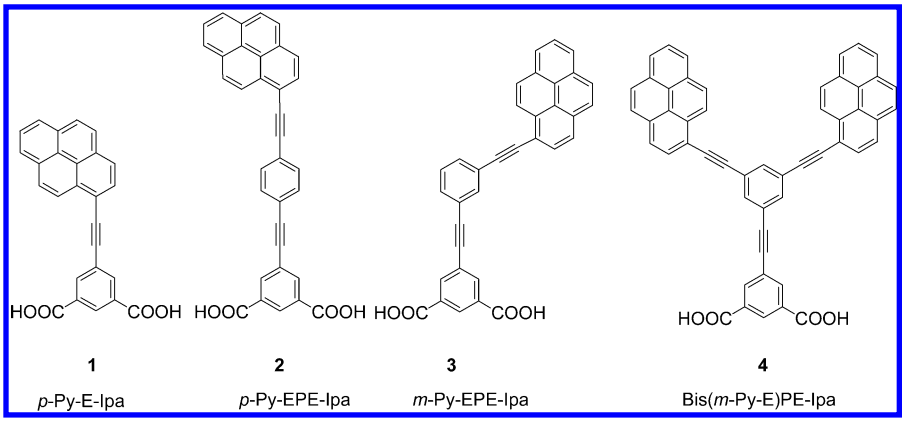


**Figure 1.** The four pyrene−spacer−anchor systems compared in this study. The ethynylene unit is abbreviated E, the *meta*- or *para*-phenylene unit is abbreviated P, and the isophthalic acid binding unit is abbreviated Ipa.

calculations to explain their fluorescence properties. In addition, the pyrene unit served as a probe for surface aggregation effects and to study the effect of excimer on charge injection.

## Experimental Section

**Metal Oxide Film Preparation.** Colloidal $TiO_2$ and $ZrO_2$ films were prepared by a previously described sol−gel technique that produces nanocrystals about ∼20 nm in diameter and mesoporous films (after sintering at 450 °C) of approximately 8−10 $\mu$m thickness.[10a] For absorption and fluorescence studies, the films were cast onto cover glass slides (VWR Scientific), for photoelectrochemical studies, the films were cast on fluorine-doped tin oxide conductive glass (FTO; Libbey-Owens-Ford), and, for electrochemical studies, the films were cast on indium−tin-oxide conductive glass (ITO). We will refer to films cast on glass or conductive glass as $TiO_2$/glass or $TiO_2$/FTO (ITO), respectively.

**Binding.** The sensitization of $TiO_2$ and $ZrO_2$ films was accomplished by immersing the films in tetrahydrofuran (THF) solutions of **1**−**4** at room temperature (RT) and letting the binding occur overnight (12−15 h). Prior to binding, the films were treated with base by immersion in a pH 11 aqueous NaOH solution for 2 min. This pretreatment was necessary to increase the surface coverage, as previously discussed.[5c] The sensitized films were rinsed thoroughly and then immersed into pure solvent until ultraviolet−visible (UV−vis) spectra showed the absence of dye desorption. The sensitized films were then used for spectroscopic or photoelectrochemical measurements. The surface coverage reached a limiting value of $\sim 8 \times 10^{-8}$ mol/cm$^2$ at ∼0.25 mM concentrations of the THF solutions of **1**−**4**.

**Adsorption Isotherms.** Surface binding of **1**−**4** was monitored spectroscopically by measuring the change in film and solution absorbance after equilibrating the film overnight in THF solutions with known concentrations of the sensitizers. In all cases, the surface coverage saturated at an ∼0.25 mM sensitizer concentration. The equilibrium binding for all sensitizers were well described by the Langmuir adsorption isotherm model[10] from which surface binding constants ($K_{ad}$) were abstracted using eq 1,

$$\frac{[S]_{eq}}{\Gamma} = \frac{1}{K_{ad}\Gamma_0} + \frac{[S]_{eq}}{\Gamma_0} \quad (1)$$

where $[S]_{eq}$ is the equilibrium concentration of the sensitizer (**1**−**4**), $\Gamma_0$ is the saturation surface coverage, and $\Gamma$ is the equilibrium surface coverage at a defined molar concentration. Plots of $[S]_{eq}/\Gamma$ versus $[S]_{eq}$ were fitted linearly to obtain the binding constants $K_{ad}$ and surface coverages $\Gamma_0$.

**Spectroscopy.** Fourier transform infrared attenuated total reflectance (FTIR−ATR) spectra were acquired on a Thermo Electron Corporation Nicolet 6700 FT-IR. UV−vis absorption spectra were acquired at an ambient temperature in THF (Acros, spectroscopic grade) using a Hewlett-Packard (HP) 8453 diode array spectrometer. Steady-state fluorescence spectra were acquired on a Spex Fluorolog that had been calibrated with a standard NIST tungsten−halogen lamp. Time-resolved fluorescence decays were acquired in THF at 373 nm excitation using a single photon-counting apparatus. Fluorescence quantum yields for the samples, $\phi_F$, were calculated in THF solutions ($\lambda = 335$ nm) with pyrene as the reference ($\phi_{Py} = 0.72$)[7] and using eq 2:

$$\phi_F = (A_{Py}/A_s)(I_s/I_{Py})(\eta_s/\eta_{Py})^2\phi_{Py} \quad (2)$$

where the subscript s refers to the samples, the subscript Py refers to pyrene, $A$ is the absorbance at the excitation wavelength, $I$ is the integrated emission area, and $\eta$ is the solvent refraction index. The radiative ($k_r$) and nonradiative ($k_{nr}$) rate constants were calculated using measured fluorescence quantum yields and lifetimes ($\tau$) and using eqs 3 and 4:

$$\phi_F = k_r/(k_r + k_{nr}) \quad (3)$$

$$\phi_F = k_r\tau \quad (4)$$

**Electrochemistry.** Cyclic voltammetry was performed with a BAS potentiostat under an atmosphere of nitrogen at RT with a conventional three-electrode configuration. A glassy carbon electrode (2 mm diameter) or a sensitized $TiO_2$/FTO film was used as the working electrode along with a platinum wire auxiliary electrode and a $Ag^+$/AgCl reference electrode in 0.1 M $TBAClO_4/CH_3CN$ electrolyte. The potential of the $Ag^+$/AgCl electrode was referenced externally versus the ferrocene/ferrocenium ($Fc/Fc^+$) redox couple. All potentials are quoted in reference to the $Fc/Fc^+$ couple. All compounds in this study display an irreversible first oxidation both in fluid solution and when anchored to $TiO_2$ when monitored at scan rates of 100 mV/s. Since the half-wave potential ($E_{1/2}$) could not be calculated because of the absence of a cathodic peak ($E_{pc}$), the anodic peak potential ($E_{pa}$) is therefore quoted [$E_{1/2} = (E_{pa} + E_{pc})/2$]. Attempts to observe $E_{pc}$ at faster scan rates were unsuccessful.

**Photoelectrochemistry.** The photocurrent action spectra were obtained in a two-electrode sandwich cell arrangement similar to what has been previously described.[11] A 0.5 M LiI/0.05 M

$I_2$ acetonitrile solution was used as the electrolyte. Quasi-monochromatic light excitation from 400 to 600 nm was achieved with a 150 W Xe lamp coupled to a *f*/2 monochromator, and incident irradiances were typically of ~1 mW/cm$^2$.

**Calculations.** The ZINDO/S CI calculations were performed on AM1 optimized structures using the Hyperchem 7.0 computational package by Hypercube, Inc. The size of the CI calculation was adjusted to include all $\pi$-bonding and lone-pair nonbonding electrons in a given molecule.

**Synthesis.** *General.* $^1$H NMR (499.90 MHz) and $^{13}$C (124.98 MHz) spectra were recorded on a Varian INOVA 500 spectrometer at RT in the solvent indicated. The $^1$H and $^{13}$C NMR chemical shifts $\delta$ are given in ppm and were referenced to tetramethylsilane and to the central line of the solvent, respectively. Coupling constants (*J*) are reported in Hz. Fast atom bombardment high-resolution mass spectra (HRMS−FAB) were obtained at a commercial facility. gas chromatography/mass spectrometry (GC/MS) data were obtained on an HP 6890 gas chromatograph with an HP 5973 MS detector. Major ions are recorded to unit mass; intensity is parenthetically indicated as a percentage of the strongest peak. Column chromatography was performed using alumina (neutral, std activity I, 50−200 $\mu$m particle size, Sorbent Technologies) or silica gel (230−600 mesh, Sorbent Technologies), and thin-layer chromatography (TLC) using silica or alumina plates and UV detection. THF was purchased anhydrous (Acros) and then distilled under nitrogen atmosphere from sodium benzophenone ketyl.

*Procedures.* The synthesis of rigid-rods **1** and **2** has been published.[5a] The synthesis of pyrene-linkers **3** and **4**, involving a series of Pd-catalyzed cross-coupling reactions[12] starting from **5** and **10**, respectively, is shown in Scheme 1. The synthesis of **10** from 1,3,5-tribromobenzene has been published,[13] and **5** was prepared with the same procedure from 1,3-diiodobenzene.

*Monodeprotection (Step a in Scheme 1).* To an ice-cold solution of **5** (195.0 mg, 0.72 mmol) in THF (25 mL), MeLi·LiBr (0.72 mmol of 2.2 M solution in diethyl ether) was added dropwise within 20 min, under nitrogen. After the addition was completed, the solution was stirred for an additional 10 min and then poured into diluted ice-cold aqueous HCl. After extraction with diethyl ether (3 × 30 mL), the organic layer was dried over $Na_2SO_4$ (anhyd). Evaporation of the solvent in vacuo gave a crude mixture of **5** and **6** (1:1 ratio by GC/MS), which was separated by column chromatography (alumina, hexane). TLC (alumina, hexane): $R_{f6} = 0.53$. The product **6** was obtained as a colorless oil (66.0 mg, 0.33 mmol, yield: 46%). $^1$H NMR $\delta_H$ (500 MHz, $CDCl_3$): 7.62 (1 H, s), 7.45 (1 H, d, $J = 8$), 7.43 (1 H, d, $J = 8$ Hz), 7.26 (1 H, t, $J = 8$), 3.09 (1 H, s), 0.27 (9 H, s). $^{13}$C NMR $\delta_C$ (125 MHz, $CDCl_3$): 135.7, 132.1, 131.9, 128.3, 123.5, 122.3, 103.9, 95.1, 82.7, 77.8, −0.1. GC/MS (*m*/*z*): 198 (M, 22), 183 (M − 15, 100), 153 (M − 45, 6). The same procedure was used to convert **10** (265.0 mg, 0.72 mmol) into **11** (colorless oil, 85.0 mg, 0.29 mmol, yield: 40%). TLC (alumina, hexane): $R_{f11} = 0.65$. $^1$H NMR $\delta_H$ (500 MHz, $CDCl_3$): 7.55 (1 H, s), 7.51 (2 H, s), 3.08 (1 H, s), 0.25 (18 H, s). $^{13}$C NMR $\delta_C$ (125 MHz, $CDCl_3$): 135.6, 135.3, 135.1, 124.0, 123.9, 122.9, 103.4, 103.2, 96.1, 95.8, 82.1, 78.5, 0.1. GC/MS (*m*/*z*): 294 (M, 23), 279 (M − 15, 100), 132 (M − 162, 13).

*Cross-Coupling with Dimethyl 5-Iodoisophthalate (Step b in Scheme 1).* Triethylamine (10 mL) was added to a flask charged with **6** (80.0 mg, 0.4 mmol) under argon atmosphere. $Pd(dba)_2$ (11.5 mg, 0.02 mmol,), CuI (7.6 mg, 0.04 mmol), $PPh_3$ (21.0 mg, 0.08 mmol), and dimethyl 5-iodoisophthalate[14,15] (140.8 mg, 0.44 mmol) were added to the solution, and the mixture was refluxed for 4 h under argon. The reaction mixture was cooled to RT, and the solvent was evaporated in vacuo to give a crude product that was purified by silica gel column chromatography ($CH_2Cl_2$). TLC (silica gel, $CH_2Cl_2$): $R_{f7} = 0.61$. Product **7** (121.0 mg, 0.31 mmol, yield: 77%) was obtained as a white powder. mp: 124−125 °C. $^1$H NMR $\delta_H$ (500 MHz, $CDCl_3$): 8.62 (s, 1 H, C$H_{Ar}$), 8.34 (s, 2 H, C$H_{Ar}$), 7.67 (s, 1 H, C$H_{Ar}$), 7.47 (1 H, d, $J = 8$), 7.45 (1 H, d, $J = 8$), 7.31 (1 H, t, $J = 8$), 3.96 (s, 6 H, COOC$H_3$), 0.27 (s, 9 H, SiC$H_3$). $^{13}$C NMR $\delta_C$ (125 MHz, $CDCl_3$): 165.7 (*C*═O); 136.5, 135.1, 132.1, 131.5, 130.9, 130.1, 128.4, 124.1, 123.6, 122.7 (*C*H$_{Ar}$, C$_{Ar}$); 103.8, 95.2, 90.3, 87.8 (*C*≡*C*); 52.5 (2 C, COO*C*H$_3$), −0.2 (Si*C*H$_3$). GC/MS (*m*/*z*): 390 (M, 67), 375 (M − 15, 100), 172 (M − 218, 20), 150 (M − 240, 14). The same procedure was used to convert **11** (80.0 mg, 0.27 mmol) into **12** (white powder, 105.0 mg, 0.21 mmol, yield: 80%). TLC (silica gel, $CH_2Cl_2$): $R_{f12} = 0.55$. mp: 145−146 °C. $^1$H NMR $\delta_H$ (500 MHz, $CDCl_3$): 8.64 (s, 1 H, C$H_{Ar}$), 8.34 (s, 2 H, C$H_{Ar}$), 7.59 (s, 2 H, C$H_{Ar}$), 7.56 (s, 1 H, C$H_{Ar}$), 3.98 (s, 6 H, COOC$H_3$), 0.26 (s, 18 H, SiC$H_3$). $^{13}$C NMR $\delta_C$ (125 MHz, $CDCl_3$): 165.7 (*C*═O); 136.7,

**SCHEME 1 . Reagents and Conditions**[a]

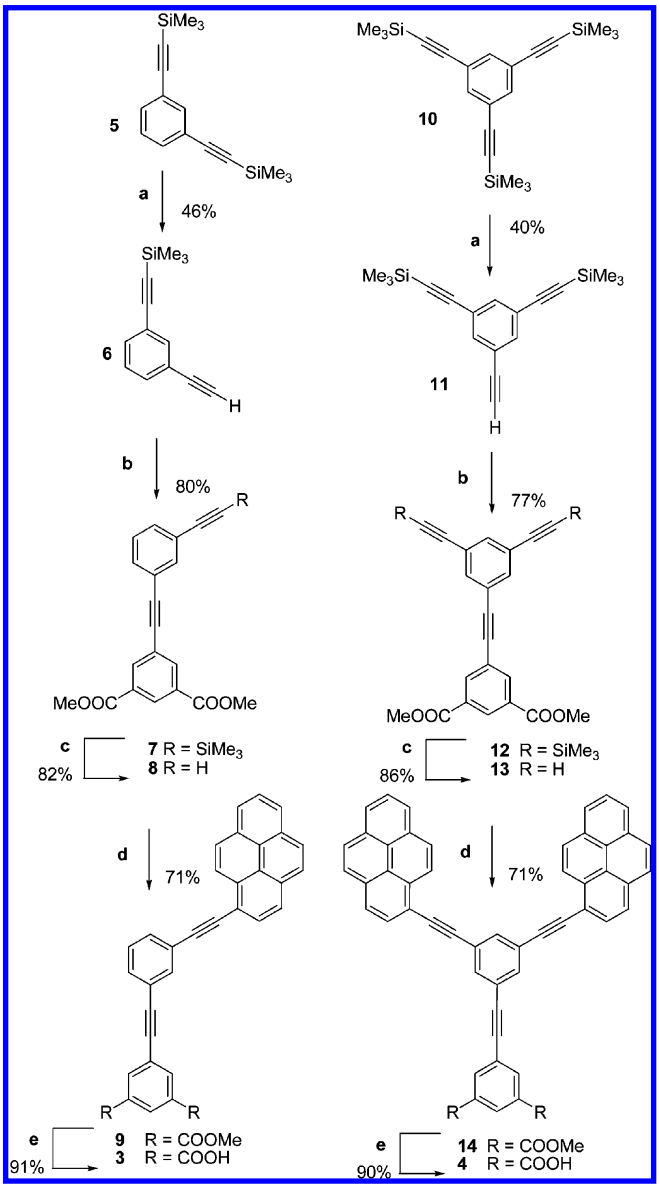


[a] Step a: MeLi·LiBr, THF, 3−5 °C. Step b: dimethyl 5-iodoisophthalate, $Pd(dba)_2$, $PPh_3$, CuI, $Et_3N$, reflux. Step c: TBAF, $CH_3CN$/$CHCl_3$, RT. Step d: 1-iodopyrene, $Pd_2(dba)_3$, P(*o*-tol)$_3$, toluene/$Et_3N$, 40 °C. Step E: (1) NaOH, $H_2O$/THF; (2) 10% HCl (aq).

135.5, 134.9, 131.2, 130.6, 124.2, 124.1, 123.2 ($CH_{Ar}$, $C_{Ar}$); 103.2, 96.2, 89.7, 88.5 ($C{\equiv}C$); 52.8 (2 C, $COOCH_3$), 0.1 (2 C, $SiCH_3$). GC/MS (*m*/*z*): 486 (M, 60), 471 (M − 15, 100), 228 (M − 258, 30).

*Deprotection of the TMS-Protected Alkyne (Step c in Scheme 1).* TBAF·$3H_2O$ (95.0 mg; 0.3 mmol) was added to a solution of **7** (100.0 mg; 0.26 mmol) in acetonitrile/chloroform (2/3, 25 mL). The reaction mixture was stirred at RT for 30 min, and then water was added. The organic layer was washed with water and brine, separated and dried over $Na_2SO_4$ (anhyd). The solvents were removed in vacuo, and the crude product was purified by silica gel column chromatography ($CH_2Cl_2$/hexane, 1/1). TLC (silica gel, $CH_2Cl_2$): $R_{f8} = 0.43$. The product **8** (70.0 mg, 0.22 mmol, yield: 86%) was obtained as a white solid. mp: 136−137 °C. $^1$H NMR $\delta_H$ (500 MHz, $CDCl_3$): 8.64 (1 H, s, $CH_{Ar}$), 8.36 (2 H, s, $CH_{Ar}$), 7.68 (1 H, s, $CH_{Ar}$), 7.52 (1 H, d, $J = 8$), 7.48 (1 H, d, $J = 8$), 7.34 (1 H, t, $J = 8$), 3.97 (6 H, s, $COOCH_3$), 3.12 (1 H, s, $C{\equiv}CH$). $^{13}$C NMR $\delta_C$ (125 MHz, $CDCl_3$) 165.6 ($C{=}O$), 136.6, 135.3, 132.4, 131.9, 131.0, 130.3, 128.6, 124.1, 122.9, 122.7 ($CH_{Ar}$, $C_{Ar}$); 90.1, 87.9, 82.6, 78.0 ($C{\equiv}C$); 52.6 (2 C, $COOCH_3$). GC/MS (*m*/*z*): 318 (M, 100), 287 (M − 31, 55), 244 (M − 74, 31). The same procedure was used to convert **12** (100.0 mg, 0.2 mmol of **12** with TBAF·$3H_2O$ 132.5.0 mg, 0.42 mmol) into **13** (white solid, 58.0 mg, 0.17 mmol, yield: 82%). TLC (silica gel, $CH_2Cl_2$): $R_{f13} = 0.53$. mp: 174−175 °C. $^1$H NMR $\delta_H$ (500 MHz, $CDCl_3$): 8.64 (s, 1 H, $CH_{Ar}$), 8.34 (s, 2 H, $CH_{Ar}$), 7.64 (s, 2 H, $CH_{Ar}$), 7.59 (s, 1 H, $CH_{Ar}$), 3.98 (s, 6 H, $COOCH_3$), 3.16 (s, 2 H, $C{\equiv}CH$). $^{13}$C APT NMR $\delta_C$ ($CDCl_3$) 165.6 ($C{=}O$), 136.7, 135.7, 135.3 ($CH_{Ar}$); 131.2 ($C_{Ar}$); 130.6 ($CH_{Ar}$); 123.8, 123.4, 123.2 ($C_{Ar}$); 89.3, 88.8 ($C{\equiv}CH$); 81.8 ($C{\equiv}C$); 79.0 ($C{\equiv}C$); 52.8 (2 C, $COOCH_3$). GC/MS (*m*/*z*): 342 (M, 100), 311 (M − 31, 45), 268 (M − 74, 15).

*Cross-Coupling with 1-Iodopyrene (Step d in Scheme 1).* A flask was charged with **8** (100.0 mg, 0.31 mmol), 1-iodopyrene[16] (114.8 mg, 0.35 mmol), $Pd_2(dba)_3$ (32.0, 0.035 mmol), and P(*o*-tol)$_3$ (85.2 mg, 0.28 mmol) in deaerated toluene/$Et_3N$ (5/1, 16 mL). The reaction mixture was stirred under argon at 40 °C. After 2 h, the reaction was complete (TLC). The solvent was evaporated in vacuo, and the crude product was purified by silica gel column chromatography ($CH_2Cl_2$). TLC (silica gel, $CH_2Cl_2$): $R_{f9} = 0.47$. The product **9** (117.1 mg, 0.23 mmol, yield: 71%) was obtained as a yellow solid. mp: 169−170 °C. $^1$H NMR $\delta_H$ (500 MHz, $CDCl_3$): 8.66 (1H, d, $J = 9$), 8.64 (1H, s), 8.39 (2H, s), 8.24 (1H, d, $J = 8$), 8.22 (1H, d, $J = 8$), 8.21 (1H, d, $J = 8$), 8.20 (1H, d, $J = 8$), 8.14 (1H, d, $J = 8$), 8.10 (1H, d, $J = 8$), 8.05 (1H, d, $J = 9$), 8.03 (1H, t, $J = 8$), 7.92 (s, 1H), 7.71 (1H, d, $J = 8$), 7.56 (1H, d, $J = 8$), 7.44 (1H, t, $J = 8$), 3.98 (6H, s). $^{13}$C NMR $\delta_C$ (125 MHz, $CDCl_3$): 165.6 ($C{=}O$), 136.6, 134.8, 132.0, 131.9, 131.5, 131.2, 131.1, 130.2, 129.7, 128.7, 128.5, 128.4, 128.3, 127.2, 126.3, 125.7, 125.7, 125.4, 124.5, 124.5, 124.3, 124.1, 124.1, 123.0, 117.4 ($CH_{Ar}$, $C_{Ar}$); 94.1, 90.4, 89.5, 88.0 ($C{\equiv}C$); 52.6 (2 C, $COOCH_3$). IR-ATR ($cm^{-1}$): 2957, 2201, 1730, 1577, 1435, 1259. The same procedure was used to react **13** (100.0 mg, 0.29 mmol) with 1-iodopyrene[16] (201.4 mg, 0.61 mmol) in the presence of $Pd_2(dba)_3$ (56.2.0 mg, 0.061 mmol) and P(*o*-tol)$_3$ (149.5 mg, 0.49 mmol) to obtain **14** (154.1 mg, 0.2 mmol, yield: 71%, yellow solid). TLC (silica gel, $CH_2Cl_2$): $R_{f14} = 0.57$. mp: 223−224 °C. $^1$H NMR $\delta_H$ (500 MHz, $CDCl_3$): 8.71 (2H, d, $J = 9$ Hz), 8.65 (1H, s), 8.38 (2H, s), 8.26 (2H, d, $J = 8$), 8.25 (2H, d, $J = 9$), 8.24 (2H, d, $J = 8$), 8.23 (2H, d, $J = 9$), 8.16 (2H, d, $J = 8.5$), 8.13 (2H, d, $J = 9$), 8.07 (2H, d, $J = 9$), 8.06 (2H, t, $J = 7.5$), 8.05 (1 H, s), 7.92 (2H, s), 3.99 (6H, s).$^{13}$C NMR $\delta_C$ (125 MHz, $CDCl_3$): 165.5 ($C{=}O$), 136.6, 134.5, 134.2, 132.1, 131.6, 131.2, 131.1, 131.0, 130.3, 129.7, 128.6, 128.4, 127.2, 126.3, 125.8, 125.7, 125.4, 124.6, 124.6, 124.5, 124.3, 123.9, 123.5, 117.1 ($CH_{Ar}$, $C_{Ar}$); 93.4, 90.2, 89.8, 88.6 ($C{\equiv}C$), 52.6 (2 C, $COOCH_3$). HRMS−FAB calcd for $C_{54}H_{31}O_4$ ($MH^+$): 743.2222. Found: 743.2225. IR-ATR ($cm^{-1}$): 3038, 2951, 2205, 1731, 1598, 1434, 1246.

*Hydrolysis: Step f in Scheme 1.* Ester **9** (20 mg, 0.039 mmol) was dissolved in THF/$H_2O$ (10 mL, 4/1), and NaOH (40 mg, 1.0 mmol) was added to the solution. The reaction mixture was stirred at r.t. for 2 h. The basic aqueous layer was extracted with chloroform, then 10% aqueous HCl was added dropwise to approximately pH 2. The precipitate was filtered and rinsed with water to afford **3** as a greenish powder (17.0 mg, 0.035 mmol, yield: 90%): $^1$H NMR $\delta_H$ (500 MHz, $CDCl_3$): 10.56 (broad s), 8.71 (1H, d, $J = 9$), 8.64 (1H, s), 8.38 (2H, s), 8.29 (1H, d, $J = 8$), 8.27 (1H, d, $J = 9$), 8.25 (1H, d, $J = 9$), 8.23 (1H, d, $J = 9$), 8.21 (1H, d, $J = 8$), 8.16 (1H, d, $J = 9$), 8.11 (1H, d, $J = 9$), 8.05 (1H, t, $J = 8$), 7.99 (1H, s), 7.75 (1H, d, $J = 8$), 7.63 (1H, d, $J = 8$), 7.50 (1H, t, $J = 8$). $^{13}$C NMR $\delta_C$ (125 MHz, $CDCl_3$): 167.33 ($C{=}O$), 137.0, 135.5, 132.9, 132.9, 132.6, 132.6, 132.4, 132.2, 131.4, 130.5, 129.8, 129.4, 129.2, 128.1, 127.2, 126.7, 126.6, 126.1, 125.5, 125.4, 125.2, 125.1, 124.7, 124.2, 120.8, 118.26 ($CH_{Ar}$, $C_{Ar}$); 94.88, 90.66, 90.11, 89.06 ($C{\equiv}C$). HRMS−FAB calcd. for $C_{34}H_{18}O_4$ ($M^+$): 490.1205. Found: 490.1213. IR-ATR ($cm^{-1}$): 3035, 2920, 2203, 1695, 1570, 1241. The same procedure was used to convert **14** (20 mg, 0.027 mmol) into **4** (17.5 mg, 0.024 mmol, yield: 91%). $^1$H NMR $\delta_H$ (500 MHz, THF): 10.84 (broad s), 8.78 (2H, d, $J = 9$ Hz), 8.68 (1H, s), 8.45 (2H, s), 8.28 (2H, d, $J = 8$ Hz), 8.27 (2H, d, $J = 9$ Hz), 8.26 (2H, d, $J = 8$ Hz), 8.25 (2H, d, $J = 9$ Hz), 8.18 (2H, d, $J = 8.5$ Hz), 8.15 (2H, d, $J = 9$ Hz), 8.14 (1H, s), 8.13 (2H, d, $J = 9$ Hz), 8.08 (2H, t, $J = 7.5$ Hz), 8.07 (2H, s). $^{13}$C NMR $\delta_C$ (125 MHz, THF): 166.4 ($C{=}O$), 137.2, 135.3, 133.2, 133.1, 133.0, 132.6, 132.3, 131.8, 131.0, 130.8, 129.8, 129.6, 128.2, 127.5, 127.0, 126.9, 126.7, 126.3, 125.9, 125.7, 125.5, 125.3, 124.6, 118.1 ($CH_{Ar}$, $C_{Ar}$); 94.3, 91.1, 90.1, 89.9 ($C{\equiv}C$). IR−ATR ($cm^{-1}$): 3335−2445, 2206, 1702, 1594, 1449, 1269, 908.

## Results and Discussion

**FTIR−ATR.** The nature of the binding of **1**−**4** to $TiO_2$ through the COOH anchoring groups of the isophthalic unit was characterized by FTIR−ATR on $TiO_2$/glass films. Figure 2 shows the IR data for compound **3**, but similar spectral changes were observed for **1**, **2**, and **4**. The nonbound **3** shows an intense asymmetric stretch $\upsilon_{(C=O)}$ at 1702 $cm^{-1}$ that is typical of the carbonyl group in carboxylic acids (Figure 2a). Upon surface binding, this band is replaced by low-energy, broad bands centered at 1594 $cm^{-1}$ (Figure 2b). Similarly to what has been observed for other rods bound to base-treated surfaces,[5c] the disappearance of the 1702 $cm^{-1}$ band and the appearance of broad bands in the carboxylate region suggest that the isophthalic anchoring portion of the dye forms bidentate (and/or monodentate) carboxylate bonds to the $TiO_2$ surface (Figure 2b, inset). Carboxylate coordination of sensitizers is generally reported for base (pH 11) pretreated or untreated $TiO_2$ thin films.[2,17] The IR spectra also show substantial changes in the region centered at ∼1250 $cm^{-1}$, as these broad bands disappear upon binding. Our studies do not allow us to identify the specific surface sites the carboxylates are coordinated to, but do indicate that both COOH groups bind as carboxylates and are present on the $TiO_2$ surface in similar environments. Carboxylate coordination to one or two $Ti^{IV}$ surface sites is consistent with these data, as shown in Figure 2b.

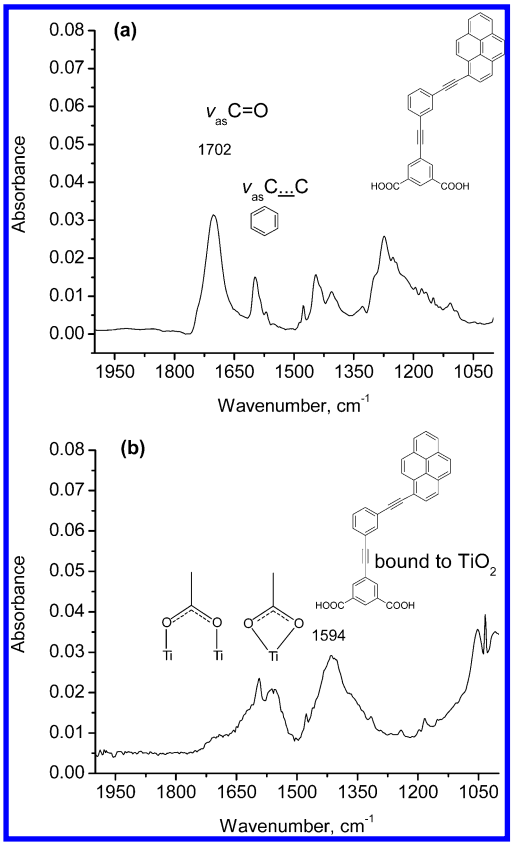


**Figure 2.** FTIR−ATR spectra of (a) **3** in the solid state and (b) **3** bound to $TiO_2$ (pH 11 pretreated).

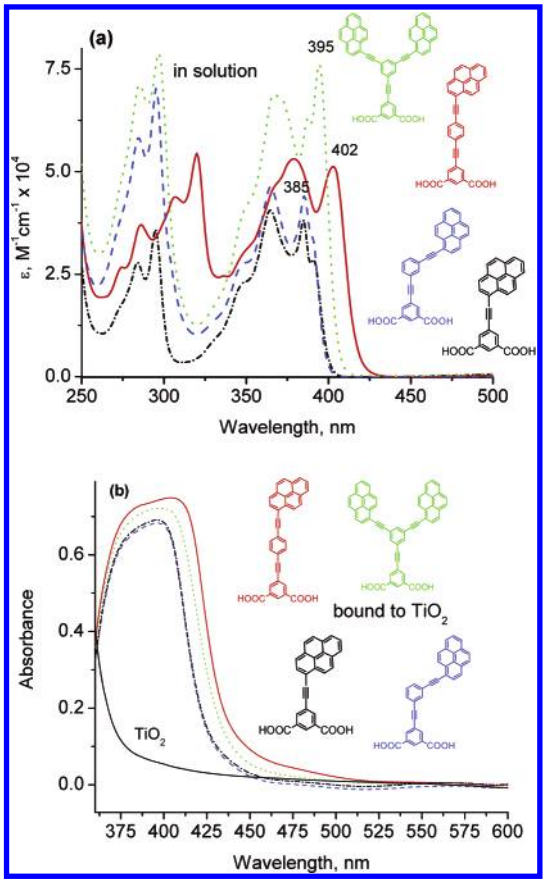


**Figure 3.** Absorption spectra of **1**−**4 (a)** in THF solution and **(b)** bound to $TiO_2$/glass. **1** (black, - · -), **2** (red, —), **3** (blue, - - -), **4** (green, ·····).

**Photophysical Studies.** The UV−vis absorbance spectra of **1**−**4** in THF solutions and bound to $TiO_2$/glass are shown in Figure 3. A comparison between these spectra allows one to observe the effects of the substitution position (meta or para) and of the number of PE units in the linker. The band at 324 nm in the spectrum of **2** was assigned to the $\pi,\pi^*$ transition of the rigid-rod $(PE)_2$ linker. The additional PE group in **2** compared to **1** (both para rigid-rods) increases the extinction coefficient and induces a ∼17 nm red shift in the long wavelength absorbance of the pyrene chromophore. Compound **3**, however, which has the same number of PE units as **2** but a meta substitution position, is blue shifted compared to the *para*-**2** by 17 nm, and its spectrum almost overlaps with the spectrum of **1**. In conclusion, an increase in PE units with para substitution is more effective in obtaining a red shift of the absorption spectrum. Introduction of a second ethynyl pyrene moiety/chromophore increases the extinction coefficient by a factor of almost 2 (**3** vs **4**).

UV−vis absorption spectra on $TiO_2$/glass (Figure 3b) were, within experimental error, identical to UV−vis absorption spectra obtained by binding on $ZrO_2$. The higher energy vibronic transitions, below 380 nm, are obscured by the fundamental absorption of the semiconductor. Only a long wavelength absorption tail into the visible was observed when 1-pyrenecarboxylic acid is anchored to pH 11 pretreated $TiO_2$, while the lowest energy vibronic component is observed for **1**−**4**.

Monochromatic irradiation (373 nm) of the pyrene compounds in THF solution at RT results in the observation of fluorescence emission. To avoid excimer formation, all samples were measured under highly dilute conditions ($10^{-6}$ M), resulting in the observation of a single emission band. Selected photophysical data are reported in Table 1. The fluorescence quantum yields were estimated using the optically dilute technique with pyrene as a standard.[7] Fluorescence decays were first-order, and the radiative ($k_r$) and nonradiative ($k_{nr}$) rate constants were calculated using eqs 3 and 4.

The introduction of PE substituents yielded a sharp, 100-fold decrease in the pyrene excited-state lifetime and was accompanied by an unexpected increase in the fluorescence quantum yield to nearly unity. This is not what would be expected upon substitution and symmetry breaking in a highly rigid aromatic hydrocarbon. Since the fluorescence quantum yields in most of these compounds exceeds 90%, radiative decay is the main deactivation pathway. In essence, they behave like good laser dyes. Such enhanced fluorescence has previously been observed by others in similarly functionalized pyrenes[9a−g] and exploited for applications in sensing.[9c] We performed a series of simple ZINDO/S configuration interaction calculations that provided useful insight into the behavior of the two lowest singlet states of pyrene upon substitution with PE groups (Table 2).[9a−e]

The calculations show that the abrupt change in the excited-state behavior results from the switching of the order of the two lowest singlet-lying states of pyrene—the forbidden $^1B_{2u}$ and the allowed $^1B_{3u}$ state[18]—rather than a simple enhancement of the transition dipole originating from the increased delocalization.[9a] The $^1B_{2u}$ lowest excited singlet state of the $D_{2h}$ unsubstituted pyrene exhibits an unusually long lifetime, which reaches hundreds of nanoseconds in carefully degassed solutions in both polar and nonpolar solvents.[7] Such a long lifetime is possible thanks to the combination of slow nonradiative decay due to the rigidity of the planar pyrene molecule and the small oscillator strength of the formally forbidden $S_1-S_0$ transition ($f = 0.002$ and $\epsilon^{371} \approx 200$ (Table 1)). Indeed, because the allowed $S_2-S_0$ transition is so much more intense ($f = 0.33$

**TABLE 1: Photophysical Properties of Compounds 1−4 and Pyrene, 1-Methyl-pyrene (Py-$CH_3$), and 1-Pyrene Carboxylic Acid (Py-COOH) Reference Compounds in THF Solution at RT**

| sensitizer | $\lambda_{abs}$, nm[a] ($\epsilon$, $M^{-1}cm^{-1}$) | $\lambda_F$,[a] nm | $\tau$,[a] ns | $\phi_F$[a] | $k_r$[a] $\times 10^8$ $s^{-1}$ | $k_{nr}$[a] $\times 10^8$ $s^{-1}$ | $E_{0-0}$, eV (nm) | $K_{ad}$ on $TiO_2$ $\times 10^5$ $M^{-1}$ | $\Gamma_{sat}$ on $TiO_2$ $\times 10^{-7}$ M $cm^{-2}$ |
|---|---|---|---|---|---|---|---|---|---|
| pyrene | 335[b] ($4.9 \times 10^4$)<br>372[c] (200) | 395 | 300 | 0.75 | 0.025 | 0.008 | 3.34 (371) | | |
| Py-$CH_3$ | 344[b] ($3.8 \times 10^4$)<br>376[c] (800) | 395 | 170 | 0.80 | 0.047 | 0.012 | 3.26 (380) | | |
| Py-COOH[d] | 351[b] ($3.2 \times 10^4$)<br>383[c] ($8.0 \times 10^3$) | 390 | 10.1 | 0.34 | 0.34 | 0.65 | 3.26 (380) | | |
| *p*-Py-E-Ipa (**1**) | 384 ($3.6 \times 10^4$) | 425 | 2.23 | 0.9 | 4.0 | 0.48 | 3.14 (395) | 0.47 | 9.8 |
| *p*-Py-EPE-Ipa (**2**) | 402 ($5.6 \times 10^4$) | 445 | 1.18 | 0.9 | 7.6 | 0.87 | 3.02 (411) | 0.83 | 5.6 |
| *m*-Py-EPE-Ipa (**3**) | 385 ($4.3 \times 10^4$) | 417 | 2.29 | 0.6 | 2.6 | 1.7 | 3.17 (391) | 0.65 | 3.9 |
| bis-(*m*-Py-E)-PE-Ipa (**4**) | 395 ($7.2 \times 10^4$) | 425 | 1.56 | 0.95 | 6.1 | 0.31 | 3.11 (399) | 1.09 | 5.9 |

[a] The methyl esters of **1**−**4** were used for solution studies because of their improved solubility in THF compared to the acids. [b] $S_2$ state [c] $S_1$ state [d] From ref 5b

**TABLE 2: Oscillator Strengths of the Lowest Spin-Allowed Transitions and Relative Radiative Decay Rates in Substituted Pyrenes Predicted by ZINDO/S CI Calculations**

| compound | three lowest spin-allowed transitions $\lambda$, nm | $f$ | calculated relative $k_r$[a] | experimental relative $k_r$[b] | CI size[c] |
|---|---|---|---|---|---|
| pyrene | 359.8 | 0.002 | 1 | 1 | 16 × 16 |
| | 326.3 | 0.565 | | | |
| | 258.3 | 0.907 | | | |
| Py-$CH_3$ | 364.3 | 0.014 | 7 | 2 | 16 × 16 |
| | 331.8 | 0.596 | | | |
| | 260.6 | 0.885 | | | |
| Py-COOH | 367.7 | 0.124 | 58 | 14 | 22 × 22 |
| | 351.3 | 0.661 | | | |
| | 285.8 | 0.003 | | | |
| Py-C≡CH | 367.6 | 0.005 | 2.5 | | 20 × 20 |
| | 348.2 | 0.744 | | | |
| | 273.9 | 0.049 | | | |
| *p*-(PE)-pyrene | 376.3 | 1.094 | 478 | 160 | 26 × 26 |
| | 371.0 | 0.028 | | | |
| | 304.0 | 0.201 | | | |
| *p*-$(PE)_2$-pyrene | 390.3 | 1.616 | 632 | 304 | 36 × 36 |
| | 371.4 | 0.010 | | | |
| | 327.3 | 0.434 | | | |
| *m*-$(PE)_2$-pyrene | 377.8 | 1.094 | 472 | 104 | 36 × 36 |
| | 370.9 | 0.016 | | | |
| | 316.9 | 0.659 | | | |

[a] Calculated as a ratio of the oscillator strengths scaled by the $\nu^3$ frequency factor of the Einstein coefficient of spontaneous emission. [b] Calculated as $k_r/k_{r(pyrene)}$ [c] The size of the CI calculation was adjusted to include all $\pi$-bonding and lone-pair nonbonding electrons in a given molecule.

and $\epsilon^{335} = 4.9 \times 10^4$ (Table 1)), the $S_1-S_0$ absorption band is frequently overlooked because it appears as an insignificant shoulder on its stronger neighbor.[9c,d] What is also overlooked is that an excited-state lifetime well in excess of 100 ns is incompatible with extinction coefficients greater than $1 \times 10^4$ because the radiative decay alone is, in this case, faster than $1 \times 10^8$ $s^{-1}$.

Substitution of pyrene with aliphatic moieties at position 1 produces a modest increase in the oscillator strength due to the lowering of symmetry and consequently relaxes the forbiddeness of the $S_1-S_0$ transition. However, another consequence of the symmetry breaking is the even higher increase in the nonradiative decay rate, and the net result is a lower fluorescence quantum yield. Indeed, 1-pyrene carboxylic acid exhibits an excited-state lifetime of ~10 ns and a fluorescence quantum yield of 32% (Table 1). The modest increase in the intensity of the lowest electronic transition upon aliphatic substitution at position 1 is born out in the ZINDO CI calculations (Table 2). Substitution with an ethynyl moiety alone appears to have a similar effect. It is the substitution with the phenylethynyl (PE) fragment that produces sufficient perturbation of the electronic structure of pyrene to abruptly switch the order of the weakly and strongly allowed states (Table 2). While, for unsubstituted pyrene, the two lowest transitions have oscillator strengths *f* of 0.002 and 0.565, respectively, in *p*-phenylethynyl pyrene, the corresponding values are 1.094 and 0.028. The strongly allowed transition to the original $^1B_{3u}$ state becomes the lowest one and gains intensity upon further expansion of the conjugated substituent. The more than 100-fold increase of the oscillator strength of the lowest electronic transition (Table 2) indicates that the radiative decay of phenylethynyl pyrenes must be correspondingly enhanced. Naturally, the presence of the second, much weaker transition at a higher excitation energy cannot be readily detected in the absorption spectrum of *p*-(PE)-pyrene and its higher analogues because it is buried under the much more intense vibronic structure of the lowest band. The state switching explains why, despite the dramatically shortened lifetimes, the substituted pyrenes exhibit *increased* rather than decreased fluorescence quantum yields. The oscillator strengths and the relative values of $k_r$ listed in Table 2 show that the low-level CI calculations reproduce the experimentally observed trends of extinction coefficients and radiative lifetimes in a semiquantitative manner and are highly useful in helping to understand the changes in the photophysics of pyrene in response to the introduction of phenylethynyl (PE) substituents.

Fluorescence spectra of the pyrene compounds **1**−**4** bound to $ZrO_2$, an insulator that has similar morphology to semiconducting $TiO_2$, were dependent on the concentration of the sensitizing solutions. Shown in Figure 4 are fluorescence spectra of **3**/$ZrO_2$ as a function of surface coverage. At low surface coverage conditions ($2.2 \times 10^{-9}$ mol/$cm^2$), the monomer and a weak excimer emission were observed at ~425 and ~525 nm, respectively. A large increase in the excimer emission band was observed with increased surface coverage (Figure 4).

The pyrene fluorescence or excimer emission of **1**−**4** bound to $TiO_2$ was not detected. Figure 5 shows a comparison of the emission from **4** at the maximum surface coverage on $ZrO_2$ and $TiO_2$. The spectra suggest that excimers are formed intermolecularly upon binding, and therefore the molecules are packed closely on the surface of the semiconductor. The requirement for the formation of excimers of aromatic hydrocarbons such as pyrene is parallel, cofacial configuration with distances of

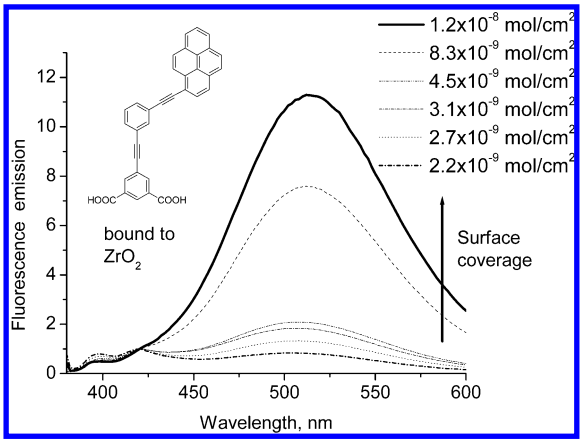


**Figure 4.** Fluorescence emission of **3** bound to $ZrO_2$/glass (normalized at 420 nm) as a function of saturation surface coverage.

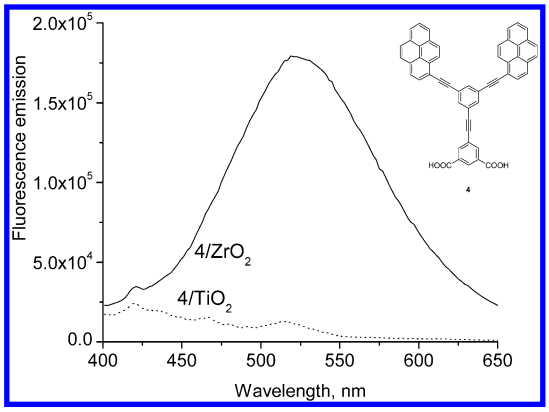


**Figure 5.** Fluorescence spectra of **4** bound to $ZrO_2$ (solid line) and to $TiO_2$ (dotted line) films at maximum surface coverage.

**TABLE 3: Anodic Peak Potentials ($E_{pa}$) of 1−4 and 1-Carboxypyrene in Solution and Bound to $TiO_2$/ITO Films vs $Fc/Fc^+$**

| sensitizer | $E_{pa}$ solution (mV) | $E_{pa}$ $TiO_2$/ITO (mV) |
|---|---|---|
| pyrene | 1230 | |
| Py-COOH | 1250 | 1340 |
| *p*-Py-E-Ipa (**1**) | 1210 | 990 |
| *p*-Py-EPE-Ipa (**2**) | 1160 | 1000 |
| *m*-Py-EPE-Ipa (**3**) | 1060 | 1130 |
| bis-(*m*-Py-E)-PE-Ipa (**4**) | 1230 | 1160 |

3−4 Å.[19] Indeed, similar behavior was observed for all pyrene−rod compounds.[5b] This fact also suggests that the pyrene excimer injects an electron into the semiconductor, effectively acting as a sensitizer. No evidence for decomposition or desorption was found by UV−vis spectroscopic measurements of the supernatant THF or of the nanoparticle thin film during the course of the experiments. However, prolonged light excitation did result in significant photochemistry.

**Electrochemistry.** Table 3 summarizes the cyclic voltammetry data recorded for pyrene, 1-pyrenecarboxylic acid and compounds **1**−**4** in solution, as well the derivatized ITO/$TiO_2$ films at a scan rate of 100 mV/s. As observed previously for unsubstituted pyrene and ethynyl pyrene systems, compounds **1**−**4** displayed irreversible redox chemistry.[9a]

The irreversible nature of this electrode process has been explained by the association of the resultant $\pi$-radical cation with a ground-state molecule to form a dimer radical cation.[9a] Compounds **1**−**4** exhibit a more negative anodic peak potential ($E_{pa}$) than that found for either pyrene or Py-COOH, thus suggesting an increase in the energy of the highest occupied molecular orbital (HOMO) of these compounds with increasing conjugation. This trend is reflected in the $E_{pa}$ potentials of Py-COOH, *p*-Py-E-Ipa (**1**) and *p*-Py-EPE-Ipa (**2**), which display $E_{pa}$ potentials of 1.25, 1.21, and 1.16 V respectively vs $Fc/Fc^+$. Compounds *m*-Py-EPE-Ipa (**3**) and bis-(*m*-Py-E)-Ipa (**4**) deviate from this trend because the meta position of the ethynylpyrene chromophore precludes conjugation with the isophthalate rigid-rod moiety. A direct comparison can be made between compounds **2** and **3** to evaluate the effect of meta or para substitution on the electronic communication between the ethynylpyrene and Ipa moieties. The lower $E_{pa}$ observed for **3** ($\Delta E_{pa} = 0.10$ V) indicates a stabilization of the HOMO for **3** with respect to **2**. This observation suggests that there is a decrease in the electron-withdrawing effect of the Ipa moiety on the ethynylpyrene unit when substituted in the meta position as opposed to the para position.

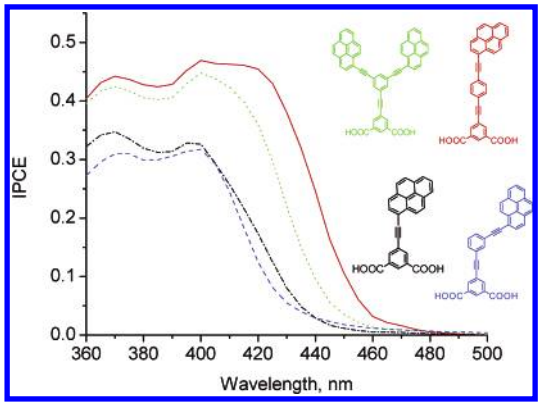


**Figure 6.** IPCE data for **1** (black, - · -), **2** (red, —), **3** (blue, - - -), and **4** (green, ·····) bound to $TiO_2$/FTO (pH 11 pretreated).

The trend observed for the para-substituted compounds **1**, **2** and **3** in acetonitrile solution is actually reversed when the compounds are bound to $TiO_2$. Electrochemical processes on $TiO_2$ have been explained in terms of self-exchange electron−hole transfer processes through the adsorbed layer of dye, where the molecules closest to the conducting glass are oxidized, and the adjacent dye molecules are then oxidized via hole transfer.[20]

**Solar Cell Performance.** Photoelectrochemical measurements were obtained for **1**−**4** bound to $TiO_2$/FTO in a two-electrode sandwich cell arrangement with 0.5 M LiI/0.05 M $I_2$ acetonitrile electrolyte. All sensitizers studied displayed relatively high incident photon-to-current efficiencies (IPCE), about 45% for **2** and **4** and 30% for **1** and **3**. When corrections were made for transmitted light and for the FTO substrates, *absorbed* photon-to-current efficiencies (APCE) were 55−85% for **1** and **2** and 30−40% for **3** and **4**. The photocurrent action spectra shown in Figure 6 agreed well with the pyrene absorbance spectra of the $TiO_2$/FTO-bound compounds. Visible light sensitization beyond 450 nm was achieved with **2**. In contrast, 1-pyrene carboxylic acid is an inefficient sensitizer that showed no measurable sensitized photocurrent at these wavelengths.

These observations, together with the fluorescence emission studies on $ZrO_2$ indicate that the excimer acts as the sensitizer. The observation of higher efficiencies with the longest pyrene-terminated PE rigid linkers is surprising, considering that the structural modification results in a 2 orders of magnitude decrease in fluorescence lifetime and an increase in the dye−semiconductor distance.

## Conclusion

The synthesis and photophysical properties of a series of conjugated pyrene compounds have been described. Interestingly,

the introduction of ethynyl-aryl substituents is accompanied by an unexpected increase in the pyrene fluorescence quantum yield to near unity and a 100-fold decrease in the excited-state lifetime. This behavior was attributed to a reversal of the order of the two lowest-lying singlet excited states and could be useful for applications in fluorescence sensing and as laser dyes.

Photoelectrochemical studies in regenerative solar cells demonstrate that the conjugated linkers dramatically improve the properties of an inefficient sensitizer like pyrene. All pyrene-terminated PE rigid linkers converted absorbed photons to an electrical current with good efficiency. The largest increase in efficiency, by a similar amount, was obtained by employing a dichromophoric compound (**4**) or a highly conjugated system (**2**), despite the increase in the dye−$TiO_2$ distance and the decrease in the excited-state lifetime. While the poor visible light harvesting by the pyrene sensitizers precludes their practical application as solar cells, these studies and the novel excimer emission demonstrate that conjugated pyrenes are useful sensitizers for fundamental studies. The excimer emission observed upon binding to insulating $ZrO_2$, for example, directly demonstrates close packing (<4 Å) of the surface-bound sensitizers.

**Acknowledgment.** The authors are grateful to the NSF-NIRT Program (Grant 0303829) for funding. We are grateful to Prashant Kamat for generous access to his laser facility at the Radiation Laboratory, University of Notre Dame. O.T. thanks Cynthia Pagba for help with the fluorescence measurements and Dong Wang for a sample of **2**.

## References and Notes

(1) Adams, D. M.; Brus, L.; Chidsey, C. E. D.; Creager, S.; Creutz, C.; Kagan, C. R.; Kamat, P. V.; Lieberman, M.; Lindsay, S.; Marcus, R. A.; Metzger, R. M.; Michel-Beyerle, M. E.; Miller, J. R.; Newton, M. D.; Rolison, D. R.; Sankey, O.; Schanze, K. S.; Yardley, J.; Zhu, X. *J. Phys. Chem. B.* **2003**, *107*, 6668−6697.

(2) Galoppini, E. *Coord. Chem. Rev.* **2004**, *248*, 1283−1297.

(3) (a) Galoppini, E.; Guo, W.; Zhang, W.; Hoertz, P. G.; Qu, P.; Meyer G. J. *J. Am. Chem. Soc.* **2002**, *124*, 7801−7811. (b) Piotrowiak, P.; Galoppini, E.; Wei, Q.; Meyer G. J.; Wiewior, P. *J. Am. Chem. Soc.* **2003**, *125*, 5278−5279. (c) Wei, Q.; Galoppini, E. *Tetrahedron* **2004**, *60*, 8497−8508. (d) Piotrowiak, P.; Galoppini, E.; Wang, D.; Myahkostupov, M. Rutgers University, unpublished results, 2006.

(4) (a) Long, B.; Nikitin, K.; Fitzmaurice, D. *J. Am. Chem. Soc.* **2003**, *125*, 5152−5160. (b) Nikitin, K.; Long, B.; Fitzmaurice, D. *Chem. Commun.* **2003**, 282−283. (c) Loewe, R. S.; Ambroise, A.; Muthukumaran, K.; Padmaja, K.; Lysenko, A. B.; Mathur, G.; Li, Q.; Bocian, D. F.; Misra, V.; Lindsey, J. S. *J. Org. Chem.* **2004**, *69*, 1453−1460. (d) Wei, L.; Padmaja, K.; Youngblood, W. J.; Lysenko, A. B.; Lindsey, J. S.; Bocian, D. F. *J. Org. Chem.* **2004**, *69*, 1461−1469.

(5) (a) Wang, D.; Schlegel, J. M.; Galoppini, E. *Tetrahedron* **2002**, *58*, 6027−6032. (b) Hoertz, P. G.; Carlisle, R. A.; Meyer G. J.; Wang D.; Piotrowiak, P.; Galoppini, E. *Nano Lett.* **2003**, *3*, 325−330. (c) Wang, D.; Mendelsohn, R.; Galoppini, E.; Hoertz, P. G.; Carlisle, R. A.; Meyer, G. J. *J. Phys. Chem. B* **2004**, *108*, 16642−16653. (d) Lamberto, M.; Pagba, C.; Piotrowiak, P.; Galoppini, E. *Tetrahedron Lett.* **2005**, *46*, 4895−4899.

(6) Kilså, K.; Mayo, E. I.; Kuciauskas, D.; Villahermosa, R.; Lewis, N. S.; Winkler, J. R.; Gray, H. B. *J. Phys. Chem. A* **2003**, *107*, 3379−3383.

(7) (a) Murov, S. L.; Carmichael, I.; Hug, G. L. *Handbook of Photochemistry*, 2nd ed.; Marcel Dekker: New York, 1993. (b) Eaton, D. F. *Pure Appl. Chem.* **1988**, *60*, 1107−1114.

(8) Sudeep, P. K.; James, P. V.; Thomas, K. G.; Kamat, P. V. *J. Phys. Chem. A* **2006**, *110*, 5642−5649.

(9) (a) Beniston, A. C.; Harriman, A.; Lawrie, D. J.; Rostron, S. A. *Eur. J. Org. Chem.* **2004**, 2272−2276. (b) Ziessel, R.; Goze, C.; Urich, G.; Césario, M.; Retailleau, P.; Harriman, A.; Rostron, J. P. *Chem.—Eur. J.* **2005**, *11*, 7366−7378. (c) Maeda, H.; Maeda, R.; Mizuno, K.; Fujimoto, K.; Shimizu, H.; Inouye, M. *Chem.—Eur. J.* **2006**, *12*, 824−831. (d) Leroy-Lhez, S.; Fages, F. *Eur. J. Org. Chem.* **2005**, 2684−2688. (e) Harriman, A.; Hissler, M.; Ziessel, R. *Phys. Chem. Chem. Phys.* **1999**, *1*, 4203−4211. (f) Thompson, A. L.; Ahn, T.-S.; Justin-Thomas, K. R.; Thayumanavan, S.; Martínez, T. J.; Bardeen, C. J. *J. Am. Chem. Soc.* **2005**, 127, 16348. (g) Yang, S.-W.; Elengovan, A.; Hwang, K.-C.; Ho, T.-I. *J. Phys. Chem. B* **2005**, *109*, 16628−16635.

(10) (a) Heimer, T. A.; D'Arcangelis, S. T.; Farzad, F.; Stipkala, J. M.; Meyer, G. J. *Inorg. Chem.* **1996**, *35*, 5319−5324. (b) Langmuir, I. *J. Am. Chem. Soc.* **1918**, *40*, 1361−1403.

(11) Argazzi, R.; Bignozzi, C. A.; Heimer, T. A.; Castellano, F. N.; Meyer, G. J. *Inorg. Chem.* **1994**, *33*, 5741−5749.

(12) (a) Stang, P. J.; Diederich, F. *Metal-Catalyzed Cross-Coupling Reactions*; Wiley-VCH: Weinheim, Germany, 1998. (b) Sonogashira, K. In *Comprehensive Organic Synthesis*; Trost, B. M., Ed.; Pergamon: Oxford, UK, 1991; Vol. 3, pp 551−561.

(13) Guo, W.; Galoppini, E.; Gilardi, R.; Rydja, G. I.; Chen, Y.-H. *Cryst. Growth Des.* **2001**, *1*, 231−237.

(14) Wolfgang, B.; Fritz, V.; Martin, N.; Heike, H. *Chem.—Eur. J.* **1999**, *5*, 345−355.

(15) Aujard, I.; Baltaze, J.-P.; Baudin, J.-B.; Cogné, E.; Ferrage, F.; Jullien, L.; Perez, E.; Prévost, V.; Qian, L. M.; Ruel, O. *J. Am. Chem. Soc.* **2001**, *123*, 8177−8188.

(16) Osamu, Y.; Kenichi, S.; Hitochi, M.; Kazuya, N.; Tatsuhiko, F.; Kazuki, N.; Takahiro, K.; Yoshiteru, S. *Chem. Lett.* **2004**, *33*, 40−41. We prepared 1-iodopyrene by reacting 1-bromopyrene with *tert*-BuLi followed by quenching with iodine.

(17) (a) Argazzi, R.; Bignozzi, C. A.; Heimer, T. A.; Castellano, F. N.; Meyer, G. J. *Inorg. Chem.* **1994**, *33*, 5741−5749. (b) Keis, K.; Bauer, C.; Boschloo, G.; Hagfeldt, A.; Westermark, K.; Rensmo, H.; Siegbahn, H. *J. Photochem. Photobiol. A* **2002**, *148*, 57−64. (c) Strommen, D. P.; Mallick, P. K.; Danzer, G. D.; Lumpkin, R. S.; Kincaid, J. R. *J. Phys. Chem.* **1990**, *94*, 1357−1366. (d) Goff, A. H.-L.; Joiret, S.; Falaras, P. *J. Phys. Chem. B* **1999**, *103*, 9569−9575.

(18) Bito, Y.; Shida, N.; Toru, T. *Chem. Phys. Lett.* **2000**, *328*, 310−315.

(19) Birks, J. B. *Photophysics of Aromatic Molecules*; John Wiley & Sons: London, UK, 1970; pp 301−371.

(20) Bonhote, P.; Gogniat, E.; Tingry S.; Barbe, C.; Vlachopoulos, N.; Lenzmann, F.: Compte, P.; Grätzel M. *J. Phys. Chem. B* **1998**, *102*, 1498−1507.